



HAL
open science

Swirl-induced improvement of turbulent mixing: laser study in a jet-stirred tubular reactor

Anne-Marie Billet, Pascal Guiraud, Joël Bertrand

► **To cite this version:**

Anne-Marie Billet, Pascal Guiraud, Joël Bertrand. Swirl-induced improvement of turbulent mixing: laser study in a jet-stirred tubular reactor. *Chemical Engineering Science*, 1993, 48 (22), pp.3805-3812. 10.1016/0009-2509(93)80223-D . hal-01980517

HAL Id: hal-01980517

<https://hal.science/hal-01980517>

Submitted on 14 Jan 2019

HAL is a multi-disciplinary open access archive for the deposit and dissemination of scientific research documents, whether they are published or not. The documents may come from teaching and research institutions in France or abroad, or from public or private research centers.

L'archive ouverte pluridisciplinaire **HAL**, est destinée au dépôt et à la diffusion de documents scientifiques de niveau recherche, publiés ou non, émanant des établissements d'enseignement et de recherche français ou étrangers, des laboratoires publics ou privés.



OATAO is an open access repository that collects the work of Toulouse researchers and makes it freely available over the web where possible

This is an author's version published in: <http://oatao.univ-toulouse.fr/21533>

Official URL: [https://doi.org/10.1016/0009-2509\(93\)80223-D](https://doi.org/10.1016/0009-2509(93)80223-D)

To cite this version:

Billet, Anne-Marie  and Guiraud, Pascal  and Bertrand, Joël  *Swirl-induced improvement of turbulent mixing: laser study in a jet-stirred tubular reactor.* (1993) *Chemical Engineering Science*, 48 (22). 3805-3812. ISSN 0009-2509

Any correspondence concerning this service should be sent to the repository administrator: tech-oatao@listes-diff.inp-toulouse.fr

SWIRL-INDUCED IMPROVEMENT OF TURBULENT MIXING: LASER STUDY IN A JET-STIRRED TUBULAR REACTOR

A. M. DUQUENNE, P. GUIRAUD and J. BERTRAND

Laboratoire de Génie Chimique, URA CNRS 192, Ecole Nationale Supérieure d'ingénieurs de Génie Chimique, 18 Chemin de la loge, F 31078 Toulouse Cedex, France

(Received 8 February 1993; accepted for publication 19 May 1993)

Abstract— Laser measurements of local velocity and concentration in a swirling-jet stirred tubular reactor under turbulent regime provide a complete analysis of hydrodynamics and mixing processes. Comparisons with the non swirling case show how swirl promotes turbulent mixing. Local velocities are obtained by laser Doppler velocimetry. Local mixing characteristics (mean concentration and segregation) are measured by laser-induced fluorescence.

INTRODUCTION

In line mixers take accurate industrial importance in the case of rapid or instantaneous blendings since they show very few dead zones and are especially well adapted to continuous processes.

Within basic in-line mixers, products are carried by large-scale convection and turbulent diffusion: large-scale convection cuts fluids into areas and puts them into the main motion, creating big eddies; shear stresses and small-scale turbulent movements give finer vortices, in which molecular diffusion puts an end to mixing. As a consequence, turbulence has to be increased to enhance mixing.

The introduction of static mixers inside an in-line reactor may provide additional agitation of fluids. Many types of static mixers exist: baffles break the main flow and force it to change into a series of large eddies; divergent devices and elbows let fine-scale turbulence develop. Complex nozzles, jets, opposed inlets, distributors, or pulsed flows, are also promoters of turbulence and mixing.

Tubular jet-stirred mixers have been classified by Sinclair and McNaughton (1970). However, for industrial purpose, confined jets and free jets are distinguished: the former ones may be equipped by simple static mixers and the latter by nozzles that are able to speed up the mixing process. Thus, in a burner, the jet is often given a swirling effect to stabilize the flame (Bafuwa and McCallum, 1973); increasing the jet turbulence (Syred and Beer, 1974) and the dragging of the surrounding combustible gas, and promoting its blending near the nozzle and in toroidal recirculation areas—which are usual for jet flows (Barchilon and Curtet, 1964)—the swirling jet shortens the combustion length.

To analyse precisely the swirling-jet mixing process, one needs local values of velocity, energy of turbulence and concentration throughout the flow. These data would also be very useful to any modelling attempt (Guiraud *et al.*, 1992).

This paper aims to provide such local results in an in-line confined axisymmetrical swirling-jet reactor: after the report of general basis about swirling jets and the description of the experimental apparatus and techniques, these results are studied and compared to the behaviour of the corresponding non-swirling-jet mixer.

MIXING WITH A SWIRLING JET

Swirl generation

There are six main swirl generators which can be sorted out into two types: the mechanical systems such as the rotating-nozzle (So and Ahmed, 1986) and the rotating-plane distributors (Chigier and Chervinsky, 1967); and the static ones such as the twisted tape (Seymour, 1963), the purely tangential entrance (Escudier *et al.*, 1980), the tangential-radial entrance (Faler and Leibovich, 1978) and the tangential-axial one (Beer and Leuckel, 1970).

All these generators can be compared with each other. The particular high efficiency of the twisted tape has been proved (Duquenne, 1992), and anyone who is concerned with the industrial purpose may notice that this swirl generator is easy to manufacture and to adapt to a jet mixer.

Evaluation of the swirl effect

To estimate the swirl effect in a jet, the swirl number S has to be used:

$$S = \frac{G_{\theta}}{R_0 G_x} = \frac{2\pi \int_0^{R_0} \overline{\rho U(r)} \overline{W(r)} r^2 dr}{2\pi R_0 \int_0^{R_0} \overline{\rho U(r)}^2 r dr}$$

where \bar{U} and \bar{W} are, respectively, the axial and tangential velocities.

The non-dimensional number S is a significant criterion of similarity (Syred and Beer, 1974). G_{θ} notes the axial rate of angular momentum and G_x the axial

rate of axial momentum. Strictly, G_x is given by

$$G_x = 2\pi \int_0^{R_0} \rho \overline{U(r)}^2 r dr + 2\pi \int_0^{R_0} \overline{P(r)} r dr.$$

It is hardly possible to evaluate the total pressure term as it may change significantly along the nozzle, depending on how the swirl is generated. This term is therefore neglected, but the resulting error on S is minimized if the precise profiles in \overline{U} and \overline{W} at swirl generator are available (Beer and Leuckel, 1970).

Swirling-jet reactor hydrodynamics

The efficiency of swirling-jet mixers may be explained by the hydrodynamical structure of these flows. It shows four main turbulent areas which are shown in Fig. 1.

(a) *Area of jet radial expansion*: Its width can be twice the width of the free jet, even for weak swirl (when the maximal tangential velocity is 5 times weaker than the initial axial velocity U_0). Dragging, therefore mixing of surrounding fluid, is especially intense.

(b) *Toroidal recirculation zones*: These are next to the jet entrance and appear for mean swirl. They create important velocity fluctuations, which means a high level of turbulence and shear rate, and therefore a high rate of fine scale mixing.

(c) *Area of central reversed flow*: It is developed around the jet axis when the above-described toroidal zones appear. In this area, no swirl is noticed. If the initial swirl of the jet increases, axial velocity gradually decreases and eventually reaches zero on the axis (Hallet and Günter, 1984).

(d) *Recirculation zones near the wall*: These exist even for non-swirling jets. They occur symmetrically between the expanding jet and the wall. If the jet angle is large enough to make the primary flow to reach the wall as soon as it leaves the nozzle, these recirculation zones collapse.

The velocity fluctuations that these four areas promote indicate that the in-line swirling jet reactor is a rather good mixer.

Mixing with a swirling jet

Very poor information is available on swirl mixing efficiency for confined jets. Some tests (Habib and Whitelaw, 1980; Hendricks and Brighton, 1975; So and Ahmed, 1986) show that mixing occurs usually

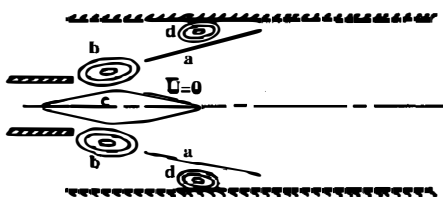


Fig. 1. Hydrodynamical structure of the swirling jet.

faster when the jet swirls intensely. However, no accurate description of the mixing process within a swirling-jet-stirred reactor has been made yet. The following section fills the gap by giving local values of velocity, turbulence and concentration in such a reactor.

EXPERIMENTAL APPARATUS AND TECHNIQUES

Apparatus

Reactor. The pilot reactor used for this study is an horizontal glass tube, the length of which is 1.8 m. Its inner radius is calibrated at $R_1 = 25 \times 10^{-3}$ m. This tube lays in a rectangular glass box full of water.

The nozzle is a tube the inner radius of which is $R_0 = 5 \times 10^{-3}$ m. It is extracted from an aluminium cylinder whose larger radius equals to R_1 exactly, and it fits perfectly the main glass tube, making sure that the nozzle is at the centre of the reactor. The nozzle length is 0.12 m.

The whole reactor is presented on Fig. 2. The z -axis begins at the outlet plane of the nozzle, and the radial coordinates are counted from the axis towards the wall.

A perfectly stirred 3 m³ tap water vessel feeds the jet. A 1 m³ one feeds the annular flow. The jet flow rate may vary from 2.78×10^{-5} to 2.78×10^{-3} m³ s⁻¹, whereas the co-current ranges from 1.94×10^{-4} to 1.17×10^{-3} m³ s⁻¹.

Swirling-jet creation. A twisted tape was introduced into the aluminium injection block. It is a piece of inox, regularly twisted around its longest axis. Its thickness is 10^{-3} m, and length 0.11 m. Once twisted, its width is exactly 10^{-2} m.

Three tapes were tested; their threads are, respectively, $pa = 0.1$, 5×10^{-2} and 4×10^{-2} m. The velocity measurements described below enable the calculation of the corresponding swirl numbers 0.17, 0.31 and 0.41, respectively. No higher swirl numbers can be obtained with twisted tapes. Smithberg and Landis (1964) did not succeed in manufacturing a twisted tape with a lower thread than $pa/R_0 = 7.2$.

Techniques. A precise investigation of velocity through the whole reactor was made possible by laser Doppler anemometry. The plane walls of the water box all around the reactor allow the laser rays to propagate from air to water without large refraction angles (Gardavsky *et al.*, 1989). The light source is

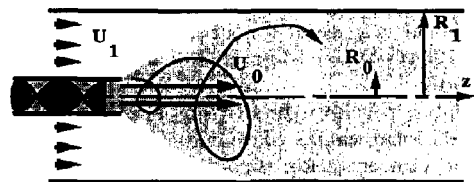


Fig. 2. Longitudinal section of the mixing apparatus.

a Spectra Physics argon ion laser (164-06) which works with maximum power of 0.5 W on the 0.488 μm line (blue). The Dantec 55X sending optics consist of a beam splitter, Bragg cell, beam expander and a 0.31 m focal lens. The Doppler signal is processed with a Dantec 55L90 counter and a Dantec 55N10 frequency shifter. The counter provides a velocity measurement when a particle goes through the probe volume. Treatment of the acceptable measurements is performed by a personal computer HP Vectra through a Dantec 92G35 numerical interface.

For the concentration measurements, jet is fed with a mixture of water and B-rhodamine, the bulk concentration being $C_0 = 5 \times 10^{-5} \text{ g l}^{-1}$. This fluorescent tracer gets excited under the 0.488 μm enlightenment and induces a fluorescent light of 0.590 μm centred spectra. The signal is converted into a voltage by constant amplification and fed to the HP Vectra computer for statistical treatment. The space resolution of this method depends only on the volume of solution from which the fluorescent light is detected. Since the characteristic time of fluorescence is very small—a few nanoseconds—the temporal resolution depends only on the electronic apparatus. The probe volume is about $0.015 \times 10^{-9} \text{ m}^3$. The light flux is converted by a Hamamatsu R955 photomultiplier and by an electronic amplifier whose constant gain is obtained using a stabilized Hamamatsu C665 supply.

Developments about the laser techniques theory were previously presented by Guiraud *et al.* (1991).

Dimensional analysis

The dimensional analysis of the system studied brings forth one geometrical and three hydrodynamical independent significant ratios.

The chosen geometrical non dimensional characteristic of the system is R_0/R_1 , which will not vary in this work. The hydrodynamical ones could be U_0/U_1 , W_{max}/U_0 and $\rho U_1 R_1/\mu$, for instance, where U_0 is the axial velocity on the axis at $z = 0$, U_1 the axial velocity of the co-current at $z = 0$, W_{max} the maximum tangential velocity in the jet outlet plane.

The variable parameters of this study are in fact U_0/U_1 , S and Re , where $Re = 2\rho U_0 R_0/\mu$ is the jet Reynolds number.

LOCAL ANALYSIS OF THE JET-STIRRED AXISYMMETRICAL TUBULAR REACTOR UNDER TURBULENT REGIME

The following description is established for $Re = 40,000$, $U_0/U_1 = 17.4$ and $S = 0.31$. The axial velocity and concentration profiles will be compared with those of a similar study dealing with the corresponding non swirling-jet reactor (Guiraud, 1989).

Axial profiles along the axis

Mean axial velocity \bar{U}/U_0 along the axis. The mean axial velocity \bar{U} , measured on the z -axis, is normalized by U_0 and plotted (Fig. 3) vs the non dimensional coordinate z/R_1 .

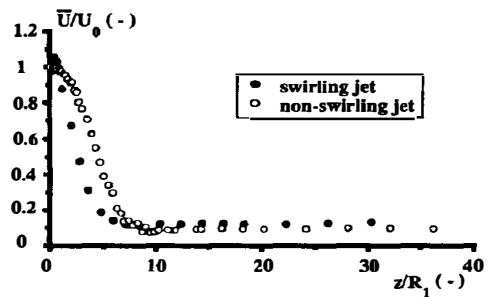


Fig. 3. Mean axial velocity axial profiles.

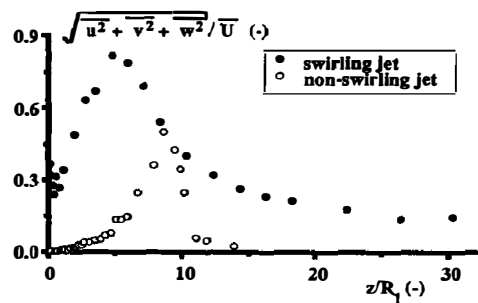


Fig. 4. Turbulence intensity axial profiles.

As soon as the jet leaves the nozzle, \bar{U} increases from U_0 to $1.1U_0$, the value that is reached at $z/R_1 = 0.5$: the jet core is slowed down along the nozzle axis because of the twisted tape wall (Duquenne, 1992). \bar{U} then goes back to the profile of a classical confined jet (Guiraud, 1989). However, the decrease of \bar{U} is observed more rapidly than in the case of a non swirling jet: \bar{U} becomes stable at $z/R_1 = 7$ instead of 8.5. The homogenization of the two flows inside the reactor operates faster when the jet swirls. This probably means that its angle of expansion is larger than that of the non swirling jet. Thanks to the swirl, a tangential velocity transient appears all around the jet, helping the usual axial velocity transient to create eddies between the two currents.

Turbulence intensity, I. A particular development of turbulence is noticed in the swirl case (Fig. 4), where profiles of turbulence intensity, I , along the z -axis are compared.

On the axis, I can be written with the relation:

$$I = \frac{(\overline{u^2} + \overline{v^2} + \overline{w^2})^{1/2}}{\bar{U}}$$

In the central region of the reactor, a high turbulence appears earlier and in a stronger way when the jet swirls, as shown by the corresponding maximum values in Fig. 4. They point out that at position z/R_1 the eddy zone, developing between the jet and its co-current, reaches the axis.

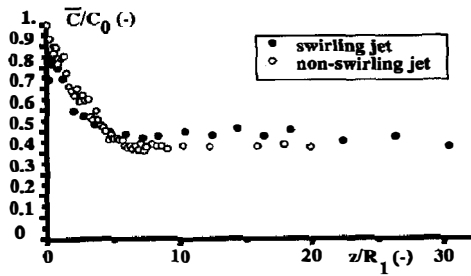


Fig. 5. Mean concentration—axial profiles.

At the end of the reactor, the remaining turbulence takes a longer time to disappear. The last value ($I = 15\%$ in the swirl case) proves that the mean flow is really turbulent.

Mean concentration, \bar{C}/C_0 . Concentration profiles are normalized by C_0 . On the axis (Fig. 5), they show two distinct parts. For the swirling jet, it is to be noted that:

—from $z/R_1 = 0$ to $z/R_1 = 7$, the mean concentration decreases quickly. It is carried by convection by the means of the radial velocities towards the annular current whose initial concentration is $\bar{C} = 0$. Turbulent diffusion is also active.

—from $z/R_1 = 7$ to the end of the reactor, the mean concentration is stable, and $\bar{C}/C_0 = 0.42$, which agrees with the mass balance in the whole mixer. At $z/R_1 = 7$, macromixing has stopped.

There is no clear difference between the profiles of mean concentration of the swirling and the non-swirling jets.

Root-mean-square concentration, $(\bar{c}^2)^{1/2}/C_0$. Since concentration is homogeneous in the jet, concentration fluctuations are quite equal to zero at $z = 0$ on the axis (Fig. 6) for both types of jets.

After jet outlet, some packets of fluids begin to be blended with the co-current all around the jet; convection and turbulent diffusion carry some pure water elements towards the axis too. That is why root-mean-square (r.m.s.) concentration increases quickly and reaches 0.15 at $z/R_1 = 1$ in the swirl case. This turbulent mixing goes on from $z/R_1 = 1$ until $z/R_1 = 9$, where concentration is probably stable through the whole reactor section. Micromixing is achieved until the scale of the probe.

At $z/R_1 = 9$, the fluctuations are very small but do not completely equal to 0: their value 0.005 is due to the noise of the measuring apparatus.

The concentration fluctuations intensity is higher if the jet swirls—0.15 instead of 0.1—and the peak arises earlier— $z/R_1 = 1.5$ instead of 4. Mixing process is promoted by the additional turbulence created by swirl.

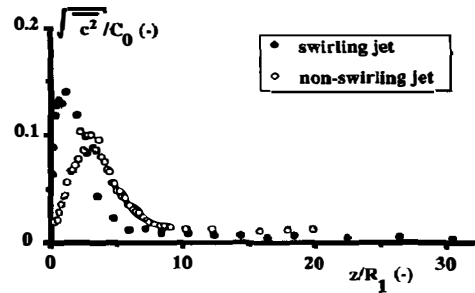


Fig. 6. R.m.s. concentration—axial profiles.

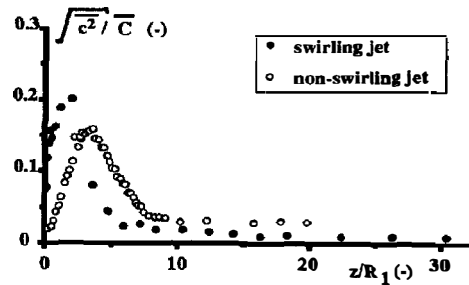


Fig. 7. Segregation intensity—axial profiles.

Segregation intensity, I_S . The segregation intensity, I_S , is defined by the following relation:

$$I_S = \frac{\sqrt{\bar{c}^2}}{\bar{C}}$$

This relative variable reveals the actual importance of local concentration fluctuations.

I_S plotted against z/R_1 , in Fig. 7, shows that the convective and turbulent diffusive actions of mixing are more efficient under swirling-jet conditions.

Once mixing is begun, I_S goes back to zero or at least to the lowest value that the experimental precision (2%) allows to be measured. I_S seems to be stable at $z/R_1 = 9$ in the swirl case and at $z/R_1 = 10$ in the classical case.

Radial profiles

We recall that the radius of the injector is $0.2R_1$.

Axial mean velocity, \bar{U}/U_0 ; expansion angles. The swirling jet spreads into its co-current flow with a larger angle than the corresponding non-swirling confined jet: two radial profiles of \bar{U}/U_0 at $z/R_1 = 2$ are drawn in Fig. 8; they show that the high values of \bar{U} that constitute the jet have already reached $r/R_1 = 0.6$ for the swirl case, whereas the non-swirling jet reaches only $r/R_1 = 0.45$. This observation agrees with the results published by Sommerfeld *et al.* (1990).

Some other profiles show the general axial flow evolution (Fig. 9): the distribution of \bar{U}/U_0 just after the nozzle exit ($z/R_1 = 0.08$) shows clearly how the jet

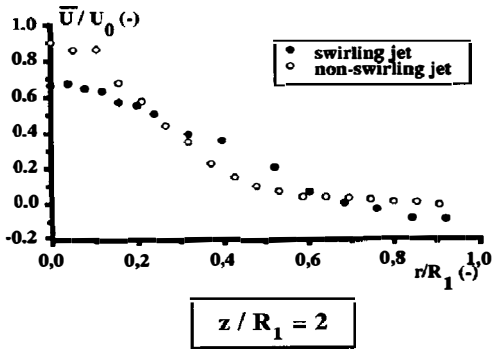


Fig. 8. Mean axial velocity radial profiles at $z/R_1 = 2$.

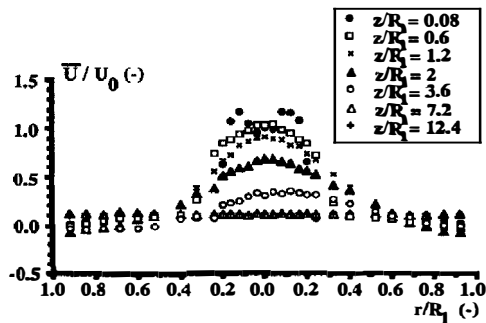


Fig. 9. Mean axial velocity radial profiles.

was slowed down all around its axis. This disturbance is noticeable for $r/R_1 < 0.08$. In this case the velocity on the axis is not the maximal one in the jet.

The boundary between the jet and its co-current is sharp when the jet leaves the nozzle. Dragging of the annular flow has not begun yet.

Six similar profiles corresponding to increasing axial coordinates are plotted in Fig. 9. At $z/R_1 = 0.6$, axial velocities near the axis have already caught up with the surrounding ones by means of the velocity transient action. Furthermore, the jet has spread from $r/R_1 = 0.24$ to $r/R_1 = 0.4$, entraining its co-current.

The following profiles show the further expansion of the jet: when it reaches the wall at $z/R_1 = 7.2$, the axial velocity distribution is flat, characterizing an axisymmetrical turbulent flow. No more transients of \bar{U} exist in the reactor.

It is observed that axial velocities are very weak near the wall; where they sometimes take negative values (at $z/R_1 = 2$ or $z/R_1 = 12$ for instance). These values indicate occasional reversed flow areas near the wall. These recirculations often appear in confined swirling jets, as stated before.

Mean radial velocity, \bar{V}/U_0 . Four profiles of \bar{V}/U_0 are set in Fig. 10. The first one ($z/R_1 = 0.6$) shows that the annular flow is entrained towards the jet: at $r/R_1 = 0.4$, \bar{V} takes negative values. The jet expands

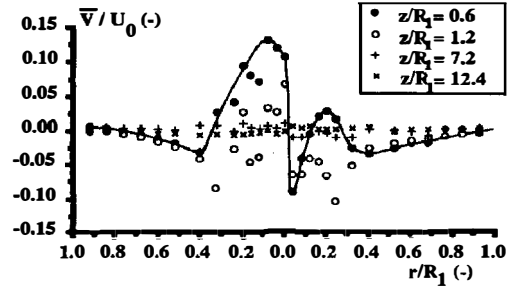


Fig. 10. Mean radial velocity radial profiles.

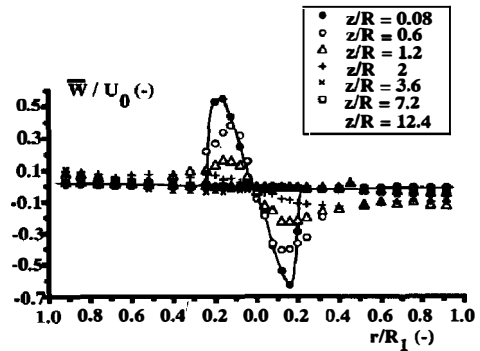


Fig. 11. Mean tangential velocity radial profiles.

towards its co-current as can be seen between $r = 0$ and $r/R_1 = 0.4$. However, the measurements at these points are not regular: weak velocities are not easy to acquire by laser anemometry. Moreover, near the axis, a small inaccuracy of rays' crossing position implies the measurement of some part of the locally high tangential velocity. Anyway, when the jet enters the reactor, velocities are disturbed by the twisted tape drag.

Radial velocities of the flow disappear after $z/R_1 = 7.2$ when axial ones homogenize. Further in the flow, no radial movements remain any more.

Mean tangential velocity, \bar{W}/U_0 . In Fig. 11 a typical distribution of \bar{W}/U_0 is plotted corresponding to $z/R_1 = 0.08$: from $r/R_1 = 0.02$ to $r/R_1 = 0.15$, \bar{W} varies linearly with r ; the flow has the "forced vortex" type. From $r/R_1 = 0.15$ to the injector wall, it has the "free vortex" type. This distribution is in very good agreement with literature (Faler and Leibovich, 1978; Escudier *et al.*, 1980).

Outside the nozzle region ($r/R_1 > 0.28$), mean tangential velocities are strictly equal to zero; at $z/R_1 = 0.08$, swirl has not propagated yet.

Further in the flow, the co-current begins to swirl; the swirl intensity thus decreases. After $z/R_1 = 3.6$, no significant tangential velocities can be measured.

Root-mean-square axial velocity, $(\bar{u}^2)^{1/2}/U_0$. The r.m.s. values of axial velocity vs non-dimensional radial

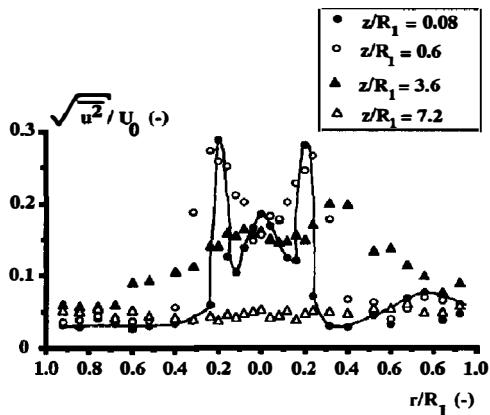


Fig. 12. R.m.s. axial velocity radial profiles.

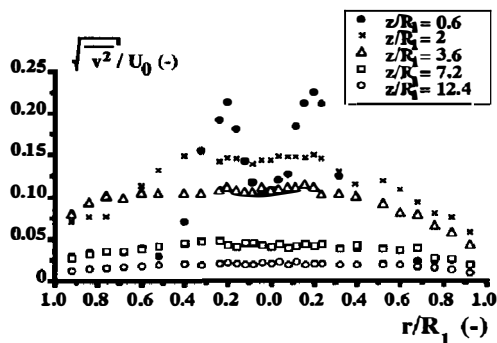


Fig. 13. R.m.s. radial velocity radial profiles.

coordinate r/R_1 are plotted in Fig. 12. At jet entrance ($z/R_1 = 0.08$) the r.m.s. axial velocity reaches a high value of $0.18U_0$, since the central low-speed zone induces some turbulence while restoring.

In the drag of the nozzle wall ($r/R_1 = 0.2$), the high fluctuations point out the local axial and tangential shear stress layers between the jet and its co-current; and the r.m.s. axial velocity equals $0.3U_0$. At $z/R_1 = 0.6$, this layer grows to reach $r/R_1 = 0.05$ near the axis and $r/R_1 = 0.4$ near the reactor wall. However, in the jet core, turbulence is restrained to 0.13. At $z/R_1 = 3.6$, axial velocity fluctuations are strong ($0.15U_0$) through the whole section of the reactor. The mean axial velocity distribution is not flat yet. At $z/R_1 = 7.2$, the r.m.s. axial velocity is lower than 0.06 through the section; it then decreases, little by little, until it reaches the usual turbulence level for such an axisymmetric turbulent flow.

Root-mean-square radial velocity, $(\overline{v^2})^{1/2}/U_0$. The r.m.s. radial velocity radial profiles (Fig. 13) are very similar to the axial velocity ones, but the maximum values are 1.5 times lower.

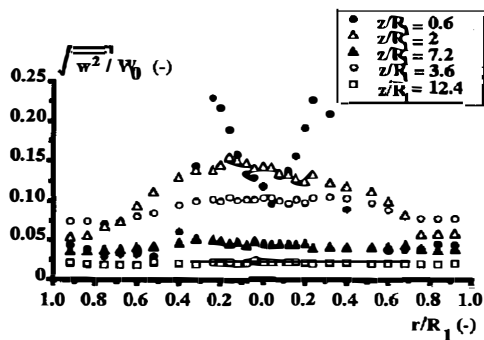


Fig. 14. R.m.s. tangential velocity radial profiles.

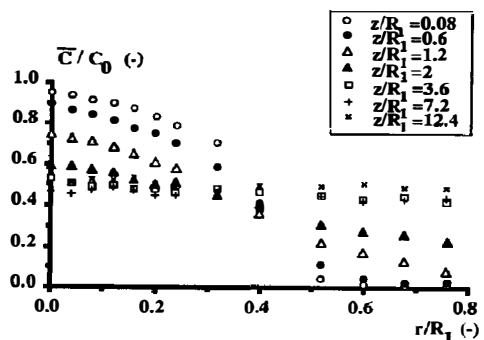


Fig. 15. Mean concentration radial profiles.

Root-mean-square tangential velocity, $(\overline{w^2})^{1/2}/U_0$. The r.m.s. tangential velocity distributions are very alike too (Fig. 14). Their peaks are intermediate between the axial and radial velocity distributions. These different values of the three components of the r.m.s. velocity at the same points show that turbulence cannot be considered as isotropic in these flows. Nevertheless, in order to model the hydrodynamical behaviour of these in-line mixers, differences are not very important and the assumption of isotropic turbulence can be made.

Turbulence intensity, I . Since mean velocities are low near the wall, the values of I are locally very important (more than 1200%). Consequently, its radial profiles are not significant.

Mean concentration, \bar{C}/C_0 . Radial profiles of \bar{C}/C_0 (Fig. 15) are plotted along the reactor radius, and not along the whole diameter, because the axisymmetry of the flow can clearly be verified on the preceding figures.

It has to be pointed out how fast the fluorescent tracer makes its way towards the annular flow. At $z/R_1 = 0.08$ it reaches $r/R_1 = 0.5$. It is extracted from the jet by both actions of convective transport and turbulent diffusion.

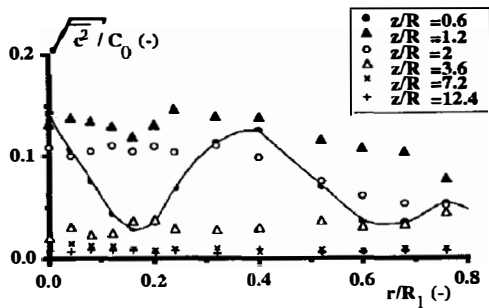


Fig. 16. R.m.s. concentration radial profiles.

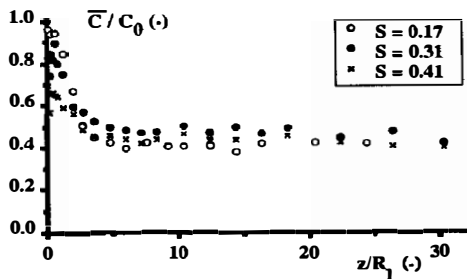


Fig. 17. Influence on mean concentration of S.

At $z/R_1 = 1.2$, the tracer is present through the whole reactor, but its mean concentration remains low for $r/R_1 > 0.4$. The distribution is flat at $z/R_1 = 7.2$.

Root mean-square concentration, $(\overline{c^2})^{1/2}/C_0$. Profiles of the r.m.s. concentration are presented in Fig. 16. At $z/R_1 = 0.6$, two peaks are noticed ($r = 0$ and $r/R_1 = 0.4$). The eddy layer between the jet and its co current has expanded towards the jet core and the wall, but pre-mixing in the central region of this layer is already achieved. Near the wall, some fluctuations appear that result from the local reversed flow areas.

Further in the reactor, fine mixing occurs through the whole section; as a result, the r.m.s. concentration is high (0.15).

At $z/R_1 = 2$, its value starts decreasing. At $z/R_1 = 3.6$, where the mean concentration is known to be almost constant through the main tube, fluctuations disappear.

Segregation intensity, I_S . Just like turbulence intensity I , I_S takes very important values near the wall of the reactor for $z/R_1 < 5$. As a consequence, no interesting information can be deduced from the radial profiles of I_S .

Influence on mixing of non dimensional parameters

It has been shown (Duquenne, 1992) that Re , in the 2000–137,000 range, has no influence on the non-dimensional variables that characterize hydrodynamics or mixing.

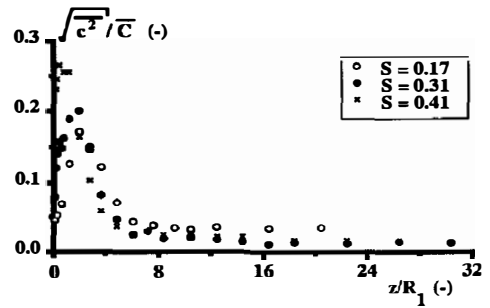


Fig. 18. Influence on segregation intensity of S.

The increase of U_0/U_1 in the 3–80 range improves the reactor performances, at least until $U_0/U_1 = 40$: above this order of magnitude no more influence is noticed (Duquenne, 1992).

As S is higher and mixing is more efficient, this assessment is proved in Figs 17 and 18 with the evolution of profiles of \overline{C}/C_0 and I_S along the axis for S varying from 0.17 to 0.41.

CONCLUSION

A swirling jet is a good mixing promoter for axisymmetrical in-line turbulent reactors. The two hydrodynamical parameters, U_0/U_1 and the swirl number, S , have an influence on its action. The higher the U_0/U_1 and S are, the faster complete mixing is reached. These points may be of significant help to enhance the performance of some industrial tubular reactors.

For this purpose, information about hydrodynamics and mixing in a jet-stirred tubular reactor under higher swirl conditions would be of great interest to check the further influence of S . Values up to $S = 2$ can be expected (Duquenne, 1992) by the means of a tangential entry for the primary flow into the injector. Moreover, S and U_0/U_1 may be used to adjust the mixing behaviour of industrial reactors involving the mixing-sensitive phenomena such as precipitation or fast chemical reactions.

However, the velocity and concentration measurements presented here can now be used as validation data for CFD (Guiraud *et al.*, 1992). A more precise description of the physical phenomenon would be provided by the measurement of cross correlations between velocity components and local concentrations. To obtain these data one must perform simultaneously the measurement of velocity and concentration in the probe volume.

Acknowledgements This work was supported by Elf-Atochem and La Grande Paroisse.

NOTATION

c	concentration fluctuation, mol m^{-3}
C	concentration of the tracer, mol m^{-3}
C_0	concentration at the exit of the jet, mol m^{-3}

G_ϕ	axial rate of angular momentum, $\text{kg m}^2 \text{s}^{-2}$
G_x	axial rate of axial momentum, kg m s^{-2}
l	turbulence intensity, dimensionless
pa	thread of twisted tapes, m
P	pressure, Pa
r	radial position, m
Re	Reynolds number of the jet: ($= 2\rho R_0 U_0/\mu$), dimensionless
R_0	radius of the jet tube, m
R_1	radius of the reactor, m
S	swirl number, dimensionless
\bar{U}	mean axial velocity, m s^{-1}
U_0	mean axial velocity at the exit of the jet, m s^{-1}
U_1	mean axial velocity at the exit of the co current, m s^{-1}
u	axial velocity fluctuation, m s^{-1}
V	radial velocity, m s^{-1}
v	radial velocity fluctuation, m s^{-1}
W	tangential velocity, m s^{-1}
W_{max}	maximal tangential velocity in the jet outlet plane, m s^{-1}
w	tangential velocity fluctuation, m s^{-1}
z	axial position, m

Greek letters

μ	dynamic viscosity, $\text{kg m}^{-1} \text{s}^{-1}$
ρ	density, kg m^{-3}

Superscript

“—” indicates a smoothed value

REFERENCES

- Bafuwa, G. C. and McCallum, N. R. L., 1973, Flame stabilization in swirling jets, in *Proceeding of the European Symposium of Combustion Institute*, pp. 565–570. Sheffield University.
- Barchilon, M. and Curtet, R., 1964, Some details of the structure of an axisymmetric confined jet with backflow. *J. Basic Engng Trans. ASME* **86**, 777–787.
- Beer, J. M. and Leuckel, W., 1970, Turbulent flames in rotating flow systems. Paper No. 7, North American Fuels Conference, Ottawa, Canada, May 1970, organized by the Canadian Combustion Institute, ASME and the Institute of Fuel.
- Chigier, N. A. and Chervinsky, A., 1967, Experimental investigation of swirling vortex motion in jets. *Trans. ASME* **E34**, 443–451.
- Duquenne, A. M., 1992, Promotion du mélange turbulent en réacteur tubulaire: jet dirigé sur un diaphragme ou jet tournant. Doctorat thesis, Institut National Polytechnique, Toulouse, France.
- Escudier, M. P., Bornstein, J. and Zehnder, N., 1980, Observations and LDA measurements of confined turbulent vortex flow. *J. Fluid Mech.* **98**, 1, 49–63.
- Faler, J. H. and Leibovich, S., 1978, An experimental map of the internal structure of a vortex breakdown, *J. Fluid Mech.* **86**, 313–335.
- Gardavsky, J., Hrbek, J., Chara, Z. and Severa, M., 1989, Refraction corrections for LDA measurements in circular tubes within rectangular optical boxes. *Dantec Inform.* **8**, 39–42.
- Guiraud, P., 1989, Mélange turbulent en réacteur tubulaire—expériences et modélisation. Doctorat thesis, Institut National Polytechnique, Toulouse, France.
- Guiraud, P., Bertrand, J. and Costes, J., 1991, Laser measurements of local velocity and concentration in a turbulent jet-stirred tubular reactor. *Chem. Engng Sci.* **46**, 1289–1297.
- Guiraud, P., Duquenne, A. M., Etcheto, L. and Bertrand, J., 1992, Numerical simulation of in-line mixers, in European Symposium on Computer Aided Process Engineering 2, 5–7 October 1992, Toulouse (France); *Comput. chem. Engng* **17S**, 511–516.
- Habib, M. A. and Whitelaw, J. H., 1980, Velocity characteristics of confined coaxial jets with and without swirl. *J. Fluid Engng Trans. ASME* **102**, 47–53.
- Hallett, W. L. H. and Günther, R., 1984, Flow and mixing in swirling flow in a sudden expansion. *Can. J. chem. Engng* **62**, 149–155.
- Hendricks, C. J. and Brighton, J. A., 1975, The prediction of swirl and inlet turbulence kinetic energy effects on confined jet mixing. *J. Fluid Engng Trans. ASME* **51**, 59.
- Seymour, E. V., 1963, A note on the improvement in performance obtainable from fitting twisted-tape turbulence promoters to tubular heat exchangers. *Trans. Instn chem. Engrs* **41**, 159–169.
- Sinclair, C. G. and McNaughton, K. J., 1970, Residence time distributions in jet stirred vessels with linear scale from 0.5 to 4 feet. *Can. J. chem. Engng* **48**, 411–419.
- Smithberg, E. and Landis, F., 1964, Friction and forced convection heat transfer characteristics in tubes with twisted tape swirl generators. *J. Heat Transfer* **86**, 39–49.
- So, R. M. and Ahmed, S. A., 1986, Effects of rotation on the flow through an axisymmetric dump combustor, in 3rd International Symposium on Applications of Laser Anemometry to Fluid Mechanics, Lisbon, Portugal, 7–9 July 1986.
- Sommerfeld, M., Qiu, H. H. and Koubaridis, D., 1990, The influence of swirl on the particle dispersion in a pipe expansion flow, in 4th International Symposium on Applications of Laser Anemometry to Fluid Mechanics, Lisbon, Portugal, 9–12 July 1990.
- Syred, N. and Beer, J. M., 1974, Combustion in swirling flows: a review. *Combust. Flame* **23**, 143–201.